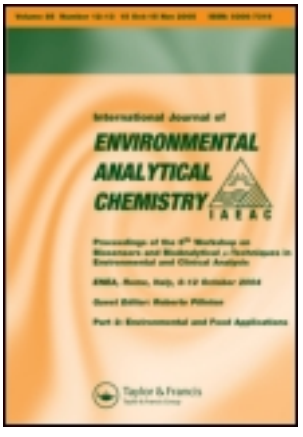

International Journal of Environmental Analytical Chemistry
Publication details, including instructions for authors and subscription information:
http://www.tandfonline.com/loi/geac20

Amperometric biosensor for hydrogen peroxide based on immobilisation of haemoglobin on mesoporous zirconia

Changhua Liu [a], Yingli Teng [a], Jing Xu [a], Yajuan Yang [a] & Zongfang Wu [a]

[a] Key Laboratory of Analytical Chemistry (Chongqing), College of Chemistry and Chemical Engineering, Southwest University, Chongqing 400700, People's Republic of China

Available online: 18 Aug 2011

To cite this article: Changhua Liu, Yingli Teng, Jing Xu, Yajuan Yang & Zongfang Wu (2011): Amperometric biosensor for hydrogen peroxide based on immobilisation of haemoglobin on mesoporous zirconia, International Journal of Environmental Analytical Chemistry, 91:14, 1367-1379

To link to this article: http://dx.doi.org/10.1080/03067319.2010.510601

Intern. J. Environ. Anal. Chem.
Vol. 91, No. 14, December 2011, 1367–1379

Taylor & Francis
Taylor & Francis Group

Amperometric biosensor for hydrogen peroxide based on immobilisation of haemoglobin on mesoporous zirconia

Changhua Liu*, Yingli Teng, Jing Xu, Yajuan Yang and Zongfang Wu

Key Laboratory of Analytical Chemistry (Chongqing), College of Chemistry and Chemical Engineering, Southwest University, Chongqing 400700, People's Republic of China

(*Received 15 December 2009; final version received 13 July 2010*)

A novel hydrogen peroxide biosensor has been presented based on fabricating mesoporous ZrO_2 and haemoglobin (mesoZrO_2-Hb) film onto gold electrode surface through coelectrodeposition. FT-IR and UV–vis spectroscopy demonstrated that haemoglobin (Hb) in the mesoporous ZrO_2 (mesoZrO_2) matrix could retain its native secondary structure. Transmission electron microscopy (TEM) image and N_2 adsorption/desorption isotherm showed that the obtained mesoZrO_2 presented disordered porous structure and appropriate pore size that was suitable for the immobilisation of Hb. The performance and factors influencing the resulting biosensor were studied in detail by means of cyclic voltammetry (CV) and chronoamperometry. Analytical parameters such as pH and applied potential were also studied. The electrochemical parameters of Hb in the mesoZrO_2 matrix were calculated with the results of the electron transfer coefficient (α) and the apparent heterogeneous electron transfer rate constant (k_s) as 0.64 and $1.47\,s^{-1}$ respectively, indicating good facilitation of the electron transfer between Hb and the modified electrode. The immobilised Hb retained its biological activity well and showed high catalytic activity to the reduction of hydrogen peroxide (H_2O_2). And the linear range was from 1.75×10^{-7} to $4.9 \times 10^{-3}\,mol\,L^{-1}$ with a detection limit of $1.0 \times 10^{-7}\,mol\,L^{-1}$ (S/N = 3). In addition, the studied biosensor exhibited high sensitivity, good reproducibility and stability.

Keywords: biosensor; haemoglobin; hydrogen peroxide; mesoporous ZrO_2

1. Introduction

The rapid and accurate determination of hydrogen peroxide (H_2O_2) is of great importance because it is an essential mediator in food, pharmaceutical, clinical, industrial and environmental analysis [1–5]. Among various analytical methods employed for hydrogen peroxide analysis, amperometric enzyme-based biosensors without mediators have aroused considerable interest due to their convenience, high sensitivity, good selectivity and quick respond to the specific substrate.

Haemoglobin (Hb) is a physiological oxygen transfer protein, consisting of four polypeptide chains, each with one electroactive iron heme group [6]. It has many advantages such as commercial availability, moderate cost, and its known and documented structure as well as its intrinsic peroxidase activity. Compared with

*Corresponding author. Email: chliu@swu.edu.cn

ISSN 0306–7319 print/ISSN 1029–0397 online

http://dx.doi.org/10.1080/03067319.2010.510601
http://www.tandfonline.com

horseradish peroxidase (HRP), Hb is much cheaper and stable in the water. Furthermore, its natural macromolecular structure lead a higher catalytic activity and longer term stability than HRP. However, facilitation of the electron transfer between Hb and electrode is relatively slow due to its electroactive centres embedded deeply in the protein structure and inaccessibility of the electroactive centre. Therefore, it is a challenge to select a host matrix to immobilise the redox protein, in which could provide a suitable microenvironment for protein and enhance the direct electron-transfer rate. Still now, various materials and methods have been developed to immobilise proteins and enzymes, such as sol–gel films [7], biopolymers [8], surfactants [9], inorganic mesoporous materials [10], nanomaterials like carbon nanotubes [11,12], MnO_2 nanosheet [13] and ZnO nanowires [14].

Among these materials, mesoporous materials are attracting great attention due to their large specific surface area, high specific pore volume, and open pore structure with pore size adjustable from 2 to 50 nm [15]. Mesoporous materials can provide confined nanospace that could stabilise proteins [16]. Moreover, enzyme immobilisation on these carriers can simply be achieved by physical adsorption which has the least effect on enzyme structures compared with other methods such as covalent bonding [17]. Therefore, they are of promising materials for the loading of biomolecules. Hitherto, several mesoporous materials were utilised for bioimmobilisation, such as mesoporous silica for haemoglobin [18,19], mesoporous tungsten oxide for haemoglobin [20], graphitised ordered macroporous carbon for haemoglobin [21,22], and the resulting biosensors have good catalytic stability and activity, and are capable of direct electrochemistry.

Mesoporous zirconia exhibits the specific pore structures and narrow pore size distributions as mesoporous materials. It also possesses excellent chemical inertness, good thermal stability, affinity for the groups containing oxygen, and biocompatibility [23]. Considering its fascinating properties, mesoporous zirconia could be used as an ideal material for protein immobilisation.

It was reported that nanoporous ZrO_2 sol-gel and polymerised thionine as mediator were used to construct a second generation biosensor by B.H. Liu and J.L. Kong *et al*. [24]. Herein, we fabricated mesoZrO_2-Hb onto gold electrode surface to construct a third generation biosensor based on coelectrodeposition. In contrast with the previous work, the immobilisation method was very simple and convenient, with minimum denaturising and strong adherence to electrode surface [25]. Electrochemical characterisation of the mesoZrO_2-Hb modified electrode was investigated and its subsequent application in the development of electrocatalytic hydrogen peroxide biosensor was studied.

2. Experimental

2.1 *Apparatus and chemicals*

Electrochemical measurements were carried out on CHI 600C electrochemical workstation (CH Instruments, Chenhua Co., Shanghai, China). The curve of UV–vis absorbance spectroscopy was performed on a UV-2205 spectrophotometer (Shimadzu, Kyoto, Japan). FT-IR spectra were obtained using a Nicolet FTIR-170SX Fourier transform infrared spectrometer (Madison, WI, USA). The morphology of mesoZrO_2 was investigated by transmission electron microscopy (TEM, JEM-100CXII, Japan). Surface area and pore characteristics of the samples were measured by BET using an AUTOSORB-1 analyser (Quantachrome AUTOSORB-1, USA).

A conventional three-electrode system was employed with a modified gold disk electrode (4.0 mm in diameter) as a working electrode, a saturated calomel electrode (SCE) as a reference electrode, and a platinum wire as an auxiliary electrode. All the potentials given in this paper were referred to the SCE. The experimental solutions were deaerated by highly pure nitrogen for 10 min, and a nitrogen atmosphere was kept over the solution during measurements.

Hb (bovine blood) was purchased from Sigma and used without further purification. Zirconium oxychloride was purchased from Tianjin Kermel Chemical Reagent Development Center, China. Cetyltrimethylammonium bromide (CTAB) was purchased from Shanghai Aladdin-reagent Co. Ammonia was purchase from Chongqing Reagent Factory, China. Hydrogen peroxide (30%, w/v solution) was purchased from Chemical Reagent Co., Chongqing, China. The concentrations of diluted H_2O_2 solutions were determined by titration with standard $KMnO_4$ solution. All other chemicals were of analytical grade. Phosphate buffer solutions (PBS, 0.1 mol L^{-1}) with various pH values were prepared by mixing stock standard solutions of K_2HPO_4 and KH_2PO_4 and adjusting the pH with H_3PO_4 or NaOH. All the solutions were prepared with doubly distilled water.

2.2 *Synthesis of mesoporous ZrO_2*

Mesoporous ZrO_2 was prepared in a typical procedure: 0.7289 g cetyltrimethylammonium bromide and 0.6445 g zirconium oxychloride was dissolved in 200 mL and 1.74 mL water, respectively. The dissolved zirconium oxychloride was added to the dissolved cetyltrimethylammonium bromide (CTAB) dropwise while stirring. After thorough mixing, ammonia was added to the mixture to adjust pH to 10 and white flocculent precipitate was produced. The white product was washed by ethanol and distilled water for three times, respectively. Then the product was dried at 110°C for 10 h in a vacuum oven. The CTAB served as template was removed by calcination at 500°C for 2 h. Consequently, the desired mesoporous ZrO_2 (mesoZrO_2) was obtained.

2.3 *Preparation of the Hb-mesoZrO_2-modified electrode*

The bare gold disk electrode was polished to a mirror-like surface with 1.0, 0.3 μm alumina slurry. The electrode was successively sonicated in ethanol and distilled water for 1 minute. Then the gold electrode was chemically cleaned by repeated potential scanning in 0.5 mol L^{-1} H_2SO_4 solution in the potential range of −0.3 to +1.5 V until the voltammogram was reproducible, and then allowed to dry. Hb solution was prepared with phosphate buffer solution (PBS). The mesoZrO_2 was dispersed in PBS (pH 6.0) to prepare 4 mg mL^{-1} mesoZrO_2 suspension. Then, 2.5 mL mesoZrO_2 suspension was mixed with 2.5 mL 5 mg mL^{-1} Hb solution (pH 6.0). Hb-mesoZrO_2/Au electrode was achieved by cycling the potential between −1.1 V and +1.6 V for 25 consecutive cycles in the mixed solution containing 2 mg mL^{-1} mesoZrO_2, 2.5 mg mL^{-1} Hb and 0.075 mol L^{-1} KCl. For comparison, a mesoZrO_2/Au electrode was prepared in a similar way. The modified electrode was stored in a refrigerator (4°C) until further use.

2.4 *Experiments of UV-vis and IR*

The mesoZrO_2 was dispersed in PBS to prepare 4 mg mL^{-1} mesoZrO_2 suspension; the mesoZrO_2 suspension was mixed with Hb solution to prepare mixed solution containing

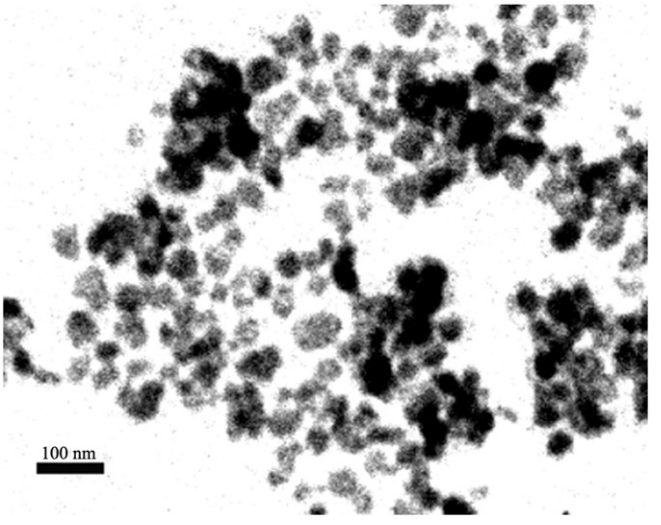

Figure 1. TEM image of mesoZrO$_2$.

2 mg mL^{-1} mesoZrO$_2$ and 2.5 mg mL^{-1} Hb. Then the curves of UV-vis absorbance were performed using a UV-2205 spectrophotometer. The mesoZrO$_2$-Hb powder was prepared by freeze drying for 12 h. Then the FT-IR of Hb, mesoZrO$_2$ and Hb-mesoZrO$_2$ was performed by a Nicolet FTIR-170SX Fourier transform infrared spectrometer.

3. Results and discussion

3.1 *Characterisation of mesoZrO$_2$ and Hb-meso ZrO$_2$*

Figure 1 displays the TEM image of mesoZrO$_2$. It can be seen that mesoZrO$_2$ possesses greatly disordered pores which have the potential capability of immobilising Hb. Figure 2 shows the surface SEM of Hb-mesoZrO$_2$/Au electrode. From Figure 2, we can conclude that Hb and mesoZrO$_2$ were immobilised on the surface of electrode. Figure 3 shows nitrogen adsorption/desorption isotherm curves of the mesoporous ZrO$_2$ before and after adsorption of Hb. The pore size distribution can be calculated through Barrett-Joyner-Halanda (BJH) model and the surface area can be estimated by applying Brunauer-Emmett–Teller (BET) equation [26,27]. The results are shown in Table 1. The average pore size is 8.6 nm, which matches well with the dimension of Hb ($5.3 \times 5.4 \times 6.5$ nm) [28]. It suggests that mesoZrO$_2$ is suitable for the immobilisation of Hb. After the immobilisation of Hb, the BET surface area, pore volume and pore size decreased obviously, indicating that Hb molecules could be incorporated into the pores of ZrO$_2$.

3.2 *Spectroscopic analysis*

UV-vis absorption spectroscopic analysis is a useful tool to probe into the secondary structure of proteins. The location of a Soret absorption band of iron heme provides information about possible denaturing of heme protein [29,30]. It can be seen that there was no obvious absorption of mesoZrO$_2$ on the absorbance band around 407 nm (curve c).

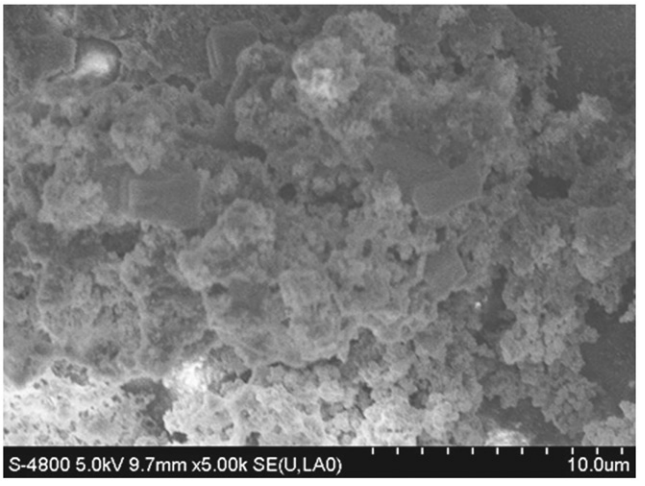

Figure 2. Surface SEM of Hb-mesoZrO_2/Au electrode.

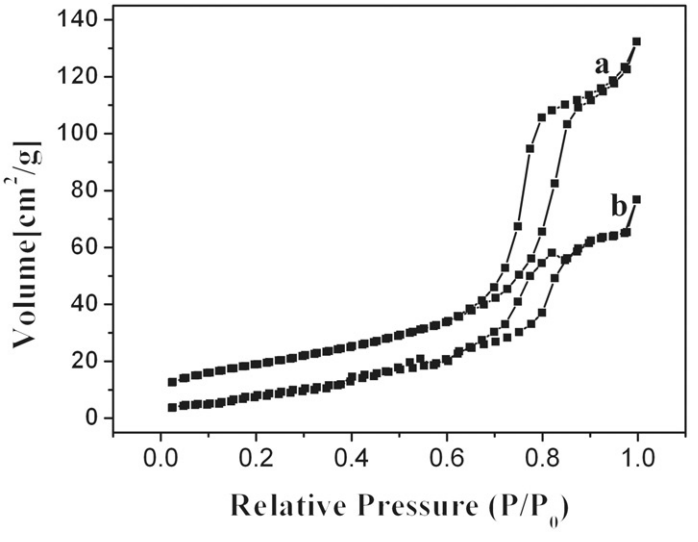

Figure 3. N_2 adsorption-desorption isotherm curves of mesoZrO_2 (a) and Hb-mesoZrO_2 (b).

Soret band of mesoZrO_2-Hb at 407 nm (Figure 4A, curve b), which was at the same position as that for the free Hb (Figure 4A, curve a), suggesting that Hb retained its native structure in mesoZrO_2-Hb.

FT-IR spectroscopy is another sensitive technique for exploring the secondary structure of proteins. As shown in Figure 4B (curve b), the infrared absorbance bands of Hb around 1652.8 and 1540.9 cm^{-1} were in correspondence to the amide I and amide II infrared adsorption bands of Hb. They can provide detailed information on the secondary structure of the polypeptide chain. The amide I band (1700–1600 cm^{-1}) was assignable to

Table 1. Pore structure parameters of mesoZrO$_2$ and Hb-mesoZrO$_2$.

Sample	S_{BET} ($m^2\,g^{-1}$)	Vads* ($cm^3\,g^{-1}$)	Vdes* ($cm^3\,g^{-1}$)	Dads* (nm)	Ddes* (nm)
mesoZrO$_2$	86.41	0.2037	0.2096	11.36	8.964
Hb-mesoZrO$_2$	60.38	0.1215	0.1326	4.151	7.9066

*Vads, Dads, pore volume and diameter calculated according to the adsorption branch of the nitrogen gas isotherm; Vdes, Ddes, pore volume and diameter calculated from the desorption branch of the nitrogen gas isotherm.

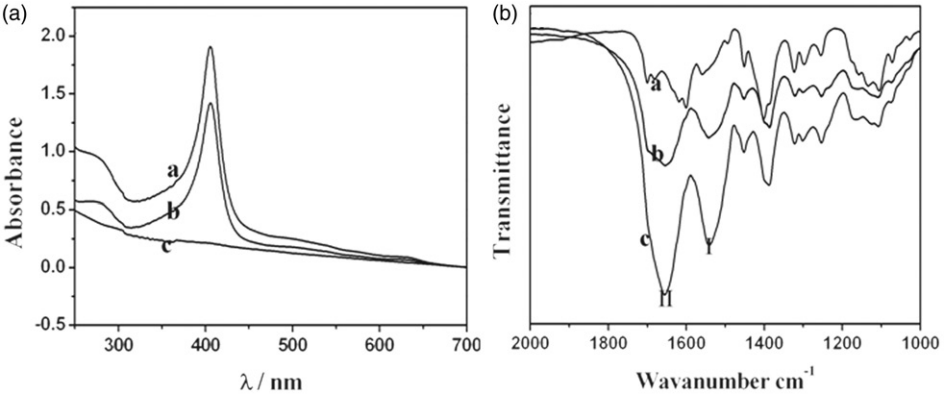

Figure 4. (A) UV-vis spectra of (a) Hb, (b) Hb/mesoZrO$_2$ and (c) mesoZrO$_2$; (B) FT-IR Spectra of (a) mesoZrO$_2$, (b) Hb and (c) Hb/mesoZrO$_2$.

C=O stretching vibrations of peptide linkages in the protein backbone. The amide II band (1620–1500 cm^{-1}) resulted from a combination of N–H bending and C–N stretching. The adsorption bands for amide I and amide II of Hb in the mesoZrO$_2$-Hb were located at 1656.6 cm^{-1} and 1542.9 cm^{-1} (Figure 4B curve c), which had a similar spectrum to that of native Hb, except a slight red shift compared to native Hb. The above results suggested that the Hb retained its native secondary structure in the mesoZrO$_2$ [31], indicating that mesoZrO$_2$ may provide a promising matrix for the enzyme immobilisation because of its satisfying biocompatibility.

3.3 *Electrochemical characteristics of the modified electrode*

The cyclic voltammetry of ferricyanide is a convenient technique to monitor the barrier of the modified electrode. The electron transfer between the solution species and the electrode must occur by tunneling either through the barrier or through the defects in the barrier. Figure 5 shows cyclic voltammograms (CVs) of different modified electrodes in 5 mmol L^{-1} ferricyanide solution. It can be seen that the bare gold electrode exhibited well-defined CVs (curve a), which was the characteristic of a diffusion-limited redox process. However, the mesoZrO$_2$/Au electrode (curve b) exhibited a decrease of the peak

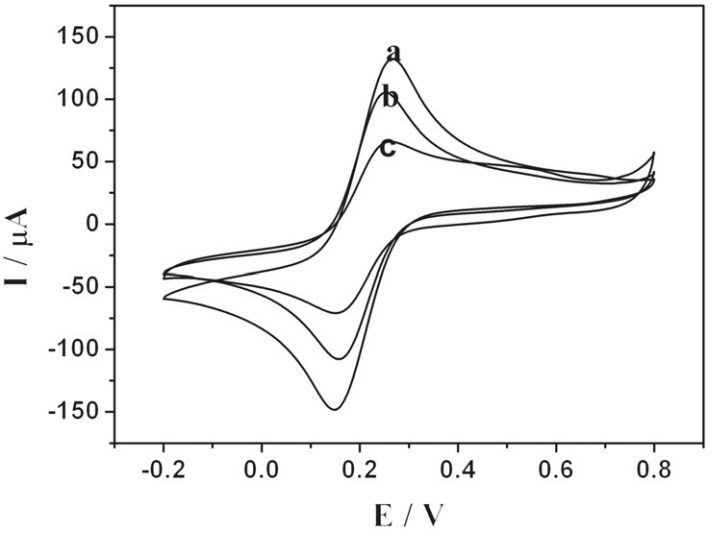

Figure 5. Cyclic voltammograms of different electrodes in 5 mmol L^{-1} $[Fe(CN)_6]^{4-/3-}$ solution (pH 7.0). (a) Bare gold disk electrode; (b) mesoZrO_2/Au electrode; (c) Hb-mesoZrO_2/Au electrode, scan rate: 100 mV s^{-1}.

current (curve b). A further decrease of peak current was observed at the mesoZrO_2-Hb/Au electrode (curve c). This decrease can be attributed to the non-conductive properties of Hb, which would obstruct electron transfer of the electrochemical probe, and confirm that Hb has been successfully immobilised onto this electrode.

The electrochemical behaviour of the Hb-mesoZrO_2/Au with different scan rate was studied. Figure 6A showed the cyclic voltammograms of Hb-mesoZrO_2/Au with different scan rate from 80 to 400 mV s^{-1}. Here, cathodic peak currents increased linearly with scan rates in the range of 100–400 mV s^{-1}, as shown in Figure 6B, suggesting a surface-controlled electrochemical behaviour. Assuming a single electron transfer reaction, the heterogeneous transfer rate constant (k_s) was estimated using the Laviron model [32] when $n\Delta E_p$ is lower than 200 mV:

$$\log k_s = \alpha \log(1-\alpha) + (1-\alpha)\log\alpha - \log\frac{RT}{nFv} - \frac{\alpha(1-\alpha)nF\Delta E_p}{2.3RT}$$

where v is the scan rate, α is the charge transfer coefficient, R is the gas constant, T is the absolute temperature, $\Delta E_p = |E_p - E'^0|$ is the difference between peak potential (E_p) and formal potential (E'^0). The E'^0 can be determined by extrapolating E_{pc} plotted versus scan rate [32]. The $E_{pc} - v$ plot exhibited a linear relationship with an intercept of −0.282 V as E'^0 (see the supplementary material, Figure 1). The plot of the peak potential versus the logarithm of the scan rates yielded a straight line (Figure 6C), from the slope of which a charge transfer coefficient of 0.64 was estimated for Hb. The k_s value was calculated to be 1.47 s^{-1} at the scan rate of 100 mV s^{-1}, which was larger than that of Hb immobilised on mesoporous silica (i.e. $0.92 \pm 0.18\ s^{-1}$) [18] and on mesoporous tungsten oxide (i.e. $0.97 \pm 0.06\ s^{-1}$) [19]. The fast electron transfer rate resulted from the strong interaction between Hb molecules and mesoZrO_2. Thus, mesoZrO_2 can provide a favourable microenvironment for Hb to undergo facile electron transfer reaction.

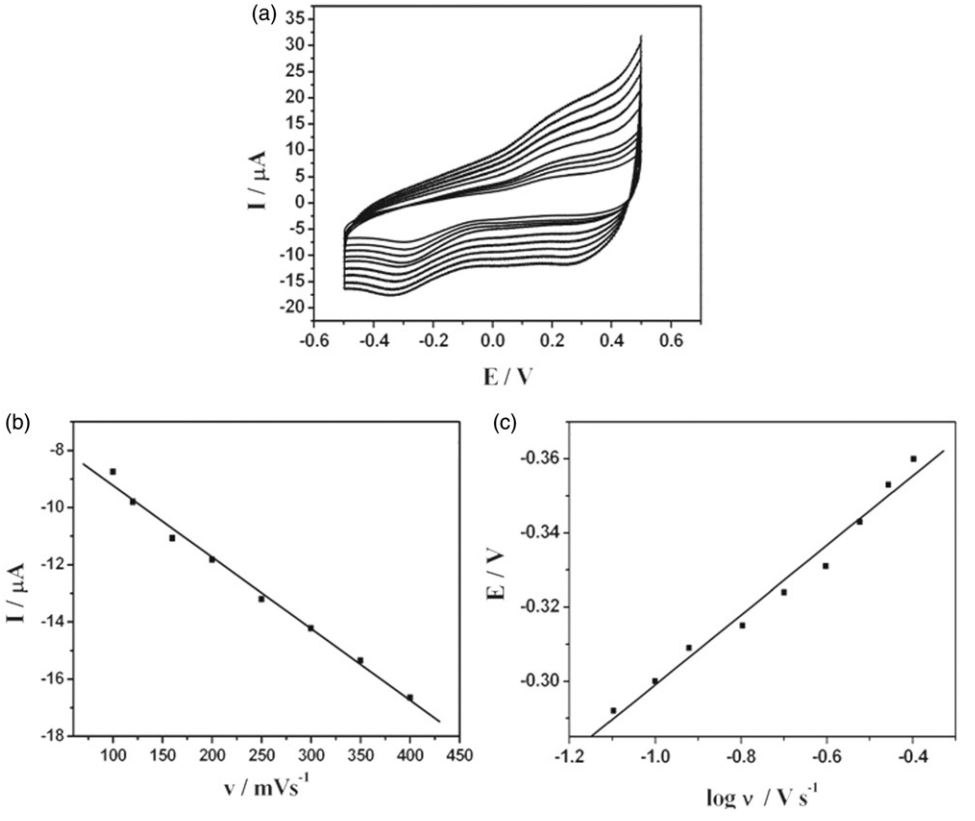

Figure 6. (A) Cyclic voltammograms of the biosensor at different scan rates (from inner to outer): 80, 100, 120, 160, 200, 250, 300, 350, 400 mV s^{-1} in 0.1 mol L^{-1} PBS (pH 7.0); (B) Plot of cathodic peak currents vs. scan rates; (C) Plot of cathodic potential vs. logarithm of scan rates.

3.4 *Electrochemical response to hydrogen peroxide of the biosensor*

The electrocatalytic reactivity of Hb-mesoZrO_2/Au electrode towards H_2O_2 was investigated by CV. Figure 7 displayed the cyclic voltammograms obtained for the biosensor in PBS (pH 7.0) containing varied concentration of H_2O_2. The catalytic reduction of hydrogen peroxide at the biosensor can be seen clearly. With the concentration of H_2O_2 changed from 1.75×10^{-4} to 3.5×10^{-4} mol L^{-1}, the cathodic current increaseed significantly, indicating a typical electrocatalytic reduction process of H_2O_2 on the modified electrode due to the direct electron transfer between Hb and electrode (Figure 7, curves b and c). The mechanism of the catalytic reduction of the immobilised Hb to H_2O_2 is exemplified by the following schemes [33]:

$$\text{Heme} - \text{Fe}^{2+} + \text{H}_2\text{O}_2 \rightarrow \text{Heme} - \text{Fe}^{3+} + \text{H}_2\text{O}$$

$$\text{Heme} - \text{Fe}^{2+} \rightarrow \text{Heme} - \text{Fe}^{3+} + \text{e}$$

3.5 *Optimisation of working conditions*

The pH value is one of the important factors for working biosensor. The effect of pH on the electrocatalytic reduction of H_2O_2 was investigated in pH range of 5.0–9.0. As shown

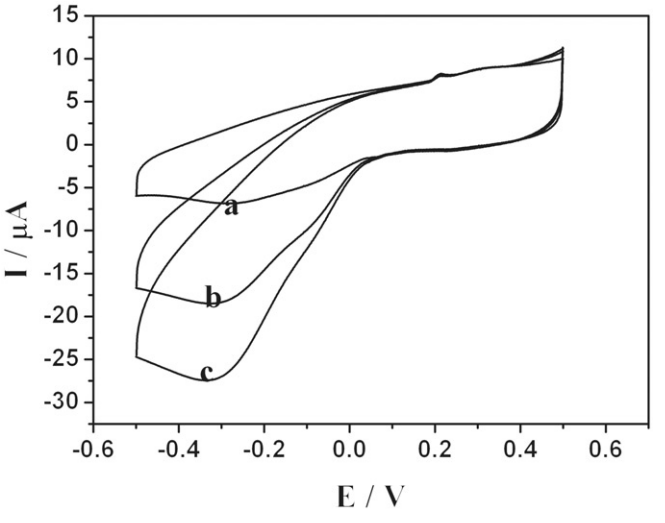

Figure 7. Cyclic voltammograms of Hb-mesoZrO_2/Au electrode with 0 (a) 1.75×10^{-4} (b) and 3.5×10^{-4} mol L^{-1} H_2O_2 (c) in 0.1 mol L^{-1} PBS (pH 7.0), scan rate: 100 mV s^{-1}.

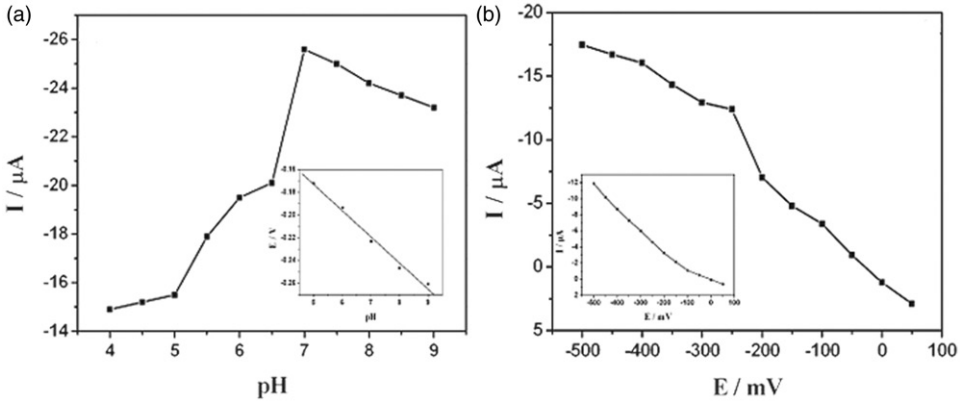

Figure 8. (A) Dependence of the current response of Hb-mesoporousZrO_2/Au electrode to 3.5×10^{-4} mol L^{-1} H_2O_2 on the pH of buffer solutions at an applied potential of −250 mV. Inset: the plot of the cathodic peak potential vs. pH; (B) Dependence of the current response of Hb-mesoporousZrO_2/Au electrode to 3.5×10^{-4} mol L^{-1} H_2O_2 on the applied potential in 0.1 M PBS (pH 7.0). Inset: Dependence of the current response of Au electrode to 3.5×10^{-4} mol L^{-1} H_2O_2 on the applied potential in 0.1 mol L^{-1} PBS (pH 7.0).

in Figure 8A, the maximum response current at the modified electrode was achieved at pH 7.0. Considering the electrochemical response and the stability of Hb, the pH 7.0 was selected as optimal pH in the following experiment. The plot of cathodic peak potential versus pH (inset in Figure 8A) showed a linear relationship with a slope of −42 mV per pH. The value was smaller than the theoretical value of −59 mV per pH for the reaction of

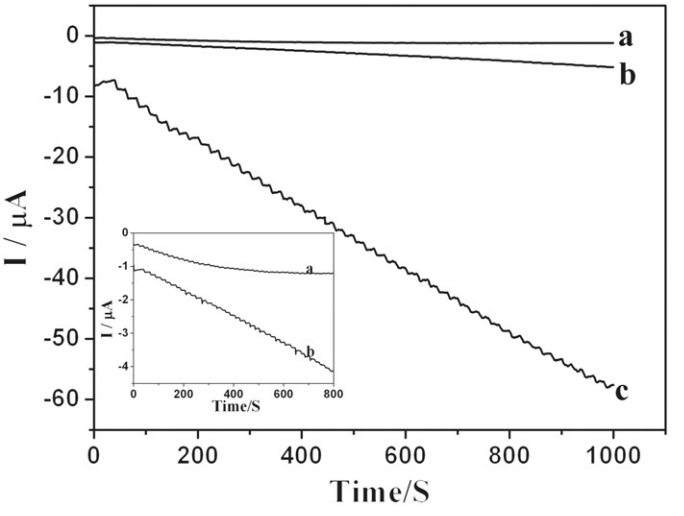

Figure 9. Amperometric responses of H_2O_2 at (a) bare gold disk electrode; (b) mesoZrO_2/Au electrode and (c) Hb-mesoZrO_2/Au electrode with successive injections of 3.5×10^{-4} mol L^{-1} H_2O_2 at the operational potential of −250 mV. Inset: Amperometric responses of H_2O_2 at (a) bare gold disk electrode and (b) mesoZrO_2/Au electrode.

one electron coupled one proton [34]. This might be due to the protonation of distal or proximal histidines, or the protonation of the water molecule coordinated to the central iron [35].

The applied potential is also an important factor for working biosensor. The influence of applied potential on bare Au and working electrode was studied (Figure 8B). The Amperometric current for bare Au electrode increased linearly from 50 mV to −500 mV (inset in Figure 8B). The amperometric current for working electrode increased sharply when the applied potential shifted from 50 mV to −250 mV, the current increased slowly when the applied potential shifted from −250 mV to −500 mV (shown in Figure 8B). The amperometric current response for working electrode was higher than that of bare Au electrode at same applied potential. These results suggested that Hb retains biocatalytic activity at mesoZrO_2. In order to obtain sufficient current response and minimise the risk for interfering reactions by other electroactive species in the solution, an applied potential of −250 mV was selected for the amperometric determination of H_2O_2.

3.6 *Performance of the hydrogen peroxide biosensor*

Amperometric responses of the bare Au electrode, mesoZrO_2/Au and mesoZrO_2-Hb/Au electrodes were investigated upon successive additions of H_2O_2 to continuously stirred PBS solution (pH 7.0) under the optimised conditions. Corresponding typical current–time curves are depicted in Figure 9. As can be seen, the bare Au electrode yielded nearly unobservable current response to H_2O_2. However, the mesoZrO_2/Au electrode displayed a detectable but very small current response to H_2O_2. But at the mesoZrO_2-Hb/Au electrode, the response current of H_2O_2 was much higher compared with bare Au electrode and mesoZrO_2/Au electrode, which indicated that Hb can directly catalyse the reduction

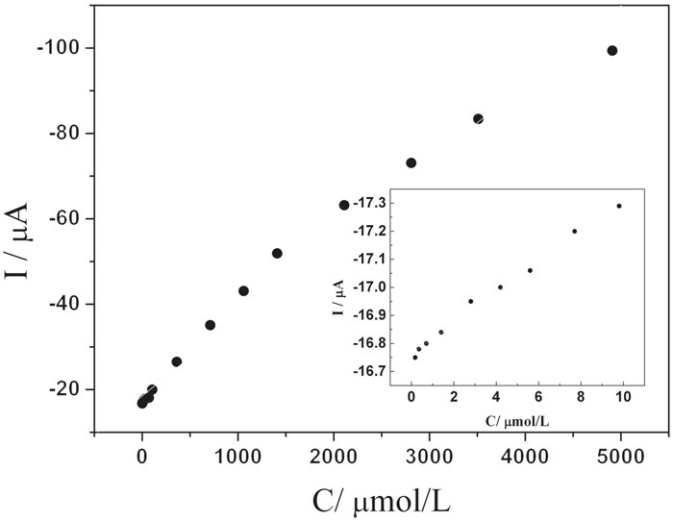

Figure 10. Linear calibration of catalytic current obtained with the Hb-mesoZrO_2/Au electrode vs. H_2O_2 concentration. Inset: the plot at low H_2O_2 concentration.

of H_2O_2 at Au electrode. In addition, the proposed biosensor achieves 95% of the steady-state current in less than 5 s, indicating a fast response process, which was due to that the mesoporous ZrO_2 could provide good microenvironment for Hb to retain its bioactivity.

Figure 10 displays the calibration plot of the biosensor. Under the optimised experimental conditions, the proposed biosensor showed a linear calibration range from 1.7×10^{-7} to 4.9×10^{-3} mol L^{-1}. The regression equation was I (μA) = −18.5–18.28c (μmol L^{-1} of H_2O_2) with a correlation coefficient of 0.990 ($n = 21$). The linear was wider than that of the sol-gel-derived nanoporous zirconia hydrogen peroxide biosensor [11]. The detection limit is 1.0×10^{-7} mol L^{-1} at 3σ which is lower than that of the hydrogen peroxide biosensor fabricate from electro-deposition ZrO_2 doped with HRP [36].

The apparent Michaelis-Menten constant (K_m^{app}) gives an indication of the enzyme-substrate kinetics, which can be obtained from the Lineweaver-Burk equation [37]:

$$1/I_{ss} = 1/I_{\max} + K_m^{app}/I_{\max}c$$

where I_{ss} is the steady-state current after the addition of a substrate and obtained from amperometric experiments, $I_{\max}$ is the maximum current under saturated substrate conditions, c is the concentration of the substrate, and K_m^{app} is the Michaelis-Menten constant. The K_m^{app} value for this H_2O_2 biosensor was calculated to be 0.39 mmol L^{-1} from Lineweaver-Burk equation. The value was lower than that on the Hb/ZrO_2/chitosan/GC electrode [38]. These results indicated that Hb molecules immobilised in mesoporous ZrO_2 retained their bioactivity and exhibit high affinity for H_2O_2.

3.7 *Repeatability, reproducibility and stability of the hydrogen peroxide biosensor*

The repeatability of the mesoZrO_2-Hb/Au was investigated. No obvious change of CV curve could be observed in the potential range from −50 mV to 50 mV with a scan rate of

Table 2. Possible interferences tested with the biosensor.

Possible interferences	Current ratio
Acetic acid	1.01
Uric acid	0.98
Ascorbic acid	1.04
L-cysteine	0.99
Glutamate	0.96
Glucose	1.00

$100\,mV\,s^{-1}$ at 0.1 mM H_2O_2 (see the supplementary material, Figure 2). The storage stability of the proposed biosensor was also studied. The biosensor was immersed in 0.1 M PBS (pH 6.0) at 4°C when not used. The response of the sensor maintained about 91% and 83% of its initial sensitivity after storage for one and two weeks at 4°C in a refrigerator when not in use, respectively. The fabrication of five electrodes was independently with the same type electrode, showed an acceptable reproducibility with a R.S.D. value of 6.2% for the catalytic current at potential of −250 mV in pH 7.0 PBS with $3.5 \times 10^{-4}\,mol\,L^{-1}$ H_2O_2.

3.8 *Selectivity of the hydrogen peroxide biosensor*

The selectivity of the biosensor was investigated by H_2O_2 determinations in the presence of some potentially coexisting compounds of H_2O_2 in biological systems. In our experiments, six interfering substances were used for measurement and the results were listed in Table 2. The current ratios were calculated by reading the current of the biosensor in the assay solution containing $3.5 \times 10^{-4}\,mol\,L^{-1}$ H_2O_2 and $7.0 \times 10^{-4}\,mol\,L^{-1}$ various interfering substance and comparing it with the current from the biosensor in the same assay solution containing only $3.5 \times 10^{-4}\,mol\,L^{-1}$ H_2O_2. The results of the current ratio illuminated that the six tested substances did not interfere significantly with the resulting biosensor for the detection of H_2O_2, which was mainly attributed to the low working potential of −250 mV used in the determination of H_2O_2 and the good anti-interference ability of the biosensor.

4. Conclusion

In this paper, an excellent biosensor was fabricated utilising mesoporous zirconia and Hb by electrodeposition. It is effectively to prevent the leakage of the protein. The newly fabricated biosensor shows fast amperometric response to H_2O_2, with high sensitivity, good stability and strong anti-interference ability. Hence the resulting electrode has potential application in the determination of H_2O_2.

References

[1] Z.Y. Wu, Z.H. Fan, Y.Y. Tang, G.L. Shen, and R.Q. Yu, Acta Chim. Sin. **64**, 738 (2006).
[2] M. Darder, K. Takada, F. Pariente, E. Lorenzo, and H.D. Abruna, Anal. Chem. **71**, 5530 (1999).
[3] J. Kulys, L. Wang, and A. Maksimoviene, Anal. Chim. Acta **274**, 53 (1993).

[4] J. Wang, Y. Lin, and L. Chen, Analyst **118**, 277 (1993).
[5] L. Wang and E.K. Wang, Electrochem. Commun. **6**, 225 (2004).
[6] M. Weissbluth, Biochem. Biophys. **15**, 68 (1974).
[7] H. Chen and S. Dong, Biosens. Bioelectron. **22**, 1811 (2007).
[8] L. Shen, R. Huang, and N. Hu, Talanta **56**, 1131 (2002).
[9] H.Y. Liu and N.F. Hu, Anal. Chim. Acta **481**, 91 (2003).
[10] L. Zhang, Q. Zhang, and J. Li, Electrochem. Commun. **9**, 1530 (2007).
[11] C.X. Cai, J. Chen. Anal. Biochem. **325**, 285 (2004).
[12] X.C. Tan, M.J. Li, P.X. Cai, L.J. Luo, and X.Y. Zou, Anal. Biochem. **337**, 111 (2005).
[13] H. Xiao, X. Chen, L.Y. Ji, X. Zhang, and W.S. Yang, Chem. Lett. **36**, 772 (2007).
[14] J.F. Zang, C.M. Li, X.Q. Cui, J.X. Wang, X.W. Sun, H. Dong, and C.Q. Sun, Electroanalysis **19**, 1008 (2007).
[15] A. Vinu, V. Murugesan, and M. Hartmann, J. Phys. Chem. B **108**, 7323 (2004).
[16] J. Kim, H. Jia, and P. Wang, Biotechnol. Adv. **24**, 296 (2006).
[17] H. Ma, J. He, D.G. Evans, and X. Duan, J. Mol. Catal. B: Enzym. **30**, 209 (2004).
[18] Z.H. Dai, S.Q. Liu, H.X. Ju, and H.Y. Chen, Biosens. Bioelectron. **19**, 861 (2004).
[19] Y.Z. Xian, Y. Xian, L.H. Zhou, F.H. Wu, Y. Ling, and L.T. Jin, Electrochem. Commun. **9**, 142 (2007).
[20] J.J. Feng, J.J. Xu, and H.Y. Chen, Electrochem. Commun. **8**, 77 (2006).
[21] X.B. Lu, Y. Xiao, Z.B. Lei, J.P. Chen, H.J. Zhang, Y.W. Ni, and Q. Zhang, J. Mater. Chem. **19**, 4707 (2009).
[22] X.B. Lu, Y. Xiao, Z.B. Lei, and J.P. Chen, Biosens. Bioelectron. **25**, 244 (2009).
[23] M.A. Aramendia, V. Borau, and C. Jimenez, J. Catal. **183**, 240 (1999).
[24] B.H. Liu, Y. Cao, D.D. Chen, J.L. Kong, and J.Q. Deng, Anal. Chim. Acta **478**, 59 (2003).
[25] Y. Itoh, M. Matsusaki, T. Kida, and M. Akashiet, Biomacromolecules **7**, 2715 (2006).
[26] E.P. Barrett, P.H. Joyner, and P.P. Halenda, J. Am. Chem. Soc. **73**, 373 (1951).
[27] S. Brunauer, P.H. Emmett, and E. Teller, J. Am. Chem. Soc. **60**, 309 (1938).
[28] S. Peng, Q. Gao, and Q. Wang, J. Shi, Chem. Mater. **16**, 2675 (2004).
[29] P. George and G. Hanania, Biochem. J. **55**, 236 (1953).
[30] H. Theorell and A. Ehrenberg, Acta Chem. Scand. **5**, 823 (1951).
[31] A.F. Nassar, W.S. Willis, and J.F. Rusling, Anal. Chem. **67**, 2386 (1995).
[32] E. Laviron, J. Electroanal. Chem. **101**, 9 (1979).
[33] A.K.M. Kafi, F. Yin, H.K. Shin, and Y.S. Kwon, Thin Solid Films **499**, 420 (2006).
[34] A.M. Bond, J. Electrochem. Soc. **127**, 528c (1980).
[35] I. Yamazaki, T. Araiso, Y. Hayashi, H. Yamada, and R. Makino, Adv. Biophys. **11**, 249 (1978).
[36] Z.Q. Tong, R. Yuan, and Y.Q. Chai, J. Biotechnol. **128**, 567 (2007).
[37] R.A. Kamin and G.S. Wilson, Anal. Chem. **52**, 1198 (1980).
[38] G. Zhao, J.J. Feng, J.J. Xu, and H.Y. Chen, Electrochem. Commun. **7**, 724 (2005).